FEBS Letters 589 (2015) 2266–2273

journal homepage: www.FEBSLetters.org

# Epigenetic harnessing of HCV via modulating the lipid droplet-protein, TIP47, in HCV cell models

Nada M. El-Ekiaby [a,*], Radwa Y. Mekky [a], Shereen A. El Sobky [b], Noha M. Elemam [a], Mohammed El-Sayed [c], Gamal Esmat [c], Ahmed I. Abdelaziz [a,*]

[a] Molecular Pathology Research Group, Department of Pharmacology and Toxicology, German University in Cairo, Cairo, Egypt
[b] Molecular Pathology Research Group, Department of Pharmaceutical Biology, German University in Cairo, Cairo, Egypt
[c] Endemic Medicine and Hepatology, Cairo University, Cairo, Egypt

ARTICLE INFO

*Article history:*
Received 24 March 2015
Revised 12 June 2015
Accepted 25 June 2015
Available online 10 July 2015

Edited by Tamas Dalmay

*Keywords:*
miR-148a
miR-30a
Tail interacting protein of 47kDa
Lipid droplets
HCV

ABSTRACT

**This study aimed at identifying potential microRNAs that modulate hepatic lipid droplets (LD) through targeting the Tail interacting protein of 47kDa (TIP47) in HCV infection.**

**Bioinformatics analysis revealed that miR-148a and miR-30a potentially target TIP47. Expression profiling showed that both microRNAs were downregulated, while TIP47 was upregulated in liver biopsies of HCV-infected patients. Forcing the expression of both microRNAs in JFH-I infected, oleic acid-treated Huh7 cells, significantly suppressed TIP47 expression and reduced cellular LDs with marked decrease in viral RNA. This study shows that miR-148a and miR-30a, regulate TIP47 expression and LDs in HCV infected cells.**



## 1. Introduction

The accumulation of lipid droplets (LDs) in the liver of HCV infected patients suggests an association between HCV infection and numerous disorders of lipid metabolism [1,2]. Moreover, cultured cells infected with HCV showed a high LD content [3]. Various viral components important for the production of new virions were found to accumulate at the surface of lipid droplets, such as the core protein, NS5A as well as +ve and −ve RNA strands [3–6]. Disruption of the association of core protein or NS5A to LDs prevents the assembly and production of infectious viral particles, which highlights the importance of the HCV–LD interaction in the viral life cycle [3,7].

Proteins associated to LDs surface, regulating their structure and function, include the family of PAT proteins, named after its three first discovered members, **P**erilipin, **A**dipocyte differentiation-related protein (ADRP), and **T**ail-interacting protein of 47 kilo Daltons (TIP47), in addition to S3-12 and OXPAT/MLDP [8–10]. The expression of PAT proteins is affected by HCV infection. In HCV core expressing cells, ADRP was found to be significantly lower, while TIP47 was significantly higher compared to cells that are not expressing the core protein [5]. However, another study showed that TIP47 protein levels were lower in HCV replicating cells compared to control cells, while its mRNA expression was higher [11]. While HCV alters TIP47 expression, TIP47 in turn is essential for HCV life cycle. Overexpression of TIP47 increased replication and release of HCV particles, while it's silencing markedly decreased the release of infectious particles. The interaction between HCV and TIP47 was reported to be through the association of NS5A to the N-terminus of TIP47 [11,12]. This interaction possibly integrates LD membranes into the HCV membranous web, facilitating HCV replication and assembly [12]. TIP47 was even found to associate to the released viral particle [13]. Recently, HCV was shown to induce hepatic LD accumulation by suppressing peroxisome proliferator-activated receptor (PPAR)-α and angiopoietin-like protein 3 (ANGPTL3), known regulators of

*Abbreviations:* LD, lipid droplet; ADRP, Adipocyte differentiation-related

*Author contributions:* Na.E., R.M. and A.A. designed the experiments; Na.E. R.M., S.E. and No.E. performed the experiments; M.E. and G.E. collected and provided the liver biopsies and patients' clinical data; Na.E. and A.A. analyzed data; Na.E. wrote the manuscript; Na.E. and A.A. made manuscript revisions.

* Corresponding authors at: Office: B5.133, German University in Cairo, The German University in Cairo – GUC, New Cairo City – Main Entrance Al Tagamoa Al Khames, 11835 Cairo, Egypt. Fax: +20 2 27581041 (A.I. Abdelaziz).

*E-mail address:* ahmed.abdel-aziz@guc.edu.eg (A.I. Abdelaziz).

http://dx.doi.org/10.1016/j.febslet.2015.06.040
0014-5793/

triglyceride homeostasis. This suppression was mediated by HCV induced upregulation of miR-27b, representing a novel mechanism contributing to the development of HCV induced hepatic steatosis [14]. Moreover, miR-27a was found to suppress HCV infection as well as cellular lipid storage in Huh7.5 cells through targeting and suppressing various lipogenic genes [15]. These data show that there is a noticeable interplay between HCV, lipid droplets along with their associated PAT proteins, and microRNAs. To date only very limited data concerning the role of microRNAs in regulating lipid droplets through regulating PAT proteins exist. Hence, this study aimed at examining the effect of microRNAs on hepatic TIP47 expression in an attempt to suppress hepatic lipid droplet formation and subsequently HCV infection.

## 2. Patients and methods

### 2.1. Patients

Liver needle biopsies were taken from 21 chronic HCV patients. All patients included are HBV negative and did not receive any treatment. Healthy liver biopsies were obtained from nine donors during liver transplantation. All patients were recruited from Al Kasr Al Aini Hospital, Cairo University Medical School. The study followed the ethical guidelines of the 1975 Declaration of Helsinki. Informed consent was obtained from all patients included in the study. Clinical parameters of the patients are presented in Table 1.

### 2.2. Cell culture

Human Hepatocellular Carcinoma cells (Huh-7) were cultured in Dulbecco's modified Eagle's medium (DMEM) supplemented with 4.5 g/L Glucose, L-Glutamine, 1% Penicillin/Streptomycin and 10% Fetal Bovine Serum (FBS). Cells were incubated in a $CO_2$ incubator adjusted to 5% $CO_2$ at 37 °C.

### 2.3. In-vitro transcription and transfection of HCV RNA

pJFH-I harboring the full-length HCV genotype 2a genome (kindly provided by Prof. Wakita) was used to generate HCV replicon cells. Briefly, pJFH-I was linearized using XbaI restriction enzyme, followed by purification of linearized DNA with phenol/chloroform. 1 μg of purified DNA was in vitro transcribed using MEGAscript® T7 Transcription Kit (Ambion, USA) yielding full length HCV RNA. 10 μg of HCV RNA were transfected into Huh7 cells using Superfect transfection reagent. 3 days post transfection, cell culture supernatant was collected, filtered using 0.45 μm filter and stored at −80 °C for later infection of naïve Huh7 cells.

**Table 1**
Patients' clinical data.

| Patient # | Age | Gender | VL | ALT | AST | Metavir score |
|---|---|---|---|---|---|---|
| P1 | 43 | M | 117744 | 28 | 30 | F1 |
| P2 | 37 | M | 1180492 | 74 | 74 | F1 |
| P3 | 36 | M | 215500 | 80 | 62 | F1 |
| P4 | 28 | F | 169000 | 32 | 25 | F1 |
| P5 | 28 | M | 106000 | 58 | 37 | F1 |
| P6 | 50 | M | 1060000 | 56 | 60 | F2 |
| P7 | 35 | F | 1650000 | 18 | 21 | F3 |
| P8 | 25 | M | 45190 | 105 | 55 | F1 |
| P9 | 47 | M | 3230000 | 26 | 28 | F3 |
| P10 | 28 | F | 119000 | 33 | 26 | F4 |
| P11 | 46 | M | 1654000 | 78 | 101 | F3 |
| P12 | 55 | M | 179000 | 76 | 80 | F3 |
| P13 | 32 | M | 3120000 | 52 | 47 | F1 |
| P14 | 35 | M | 4020000 | 74 | 65 | F1 |
| P15 | 34 | M | 1790000 | 62 | 53 | F1 |
| P16 | 52 | M | 1120000 | 34 | 53 | F4 |
| P17 | 68 | F | 15432000 | 54 | 43 | F2 |
| P18 | 34 | M | 403200 | 42 | 55 | F1 |
| P19 | 40 | F | 53200000 | 60 | 44 | F1 |
| P20 | 38 | F | 7670000 | 15 | 18 | F1 |
| P21 | 56 | F | 56300 | 67 | 53 | F4 |

### 2.4. RNA extraction and quantification

Total RNA was extracted from liver biopsies or Huh7 cells using Biozol reagent according to the manufacturer's instructions (Bioer Technology, China). The relative expression of TIP47 was quantified relative to the housekeeping gene β2-microglobulin (B2M) and the relative expression of miR-148a and miR-30a were quantified relative to the housekeeping gene RNU6B using TaqMan real-time quantitative polymerase chain reaction (PCR) (StepOne, Applied Biosystems).

### 2.5. Transfection of oligos

Huh7 cells were transfected with 25 nM mimics, antagomirs or siRNAs using Hiperfect transfection reagent (Qiagen) according to the manufacturer's instructions. Transfection was performed in 96-well plates for TIP47 mRNA quantification, intracellular LDs imaging and viral RNA quantification or in 24-well plates to examine TIP47 protein expression.

### 2.6. Fatty acid treatment

24 h post transfection with oligos; lipid loading of Huh7 cells was achieved by incubating the cells with 600 μM bovine serum albumin-coupled oleic acid (OA) (Sigma Aldrich). Cells were either harvested 48 h. after OA treatment for viral load and TIP47 mRNA quantification or after 72 h for LDs staining or protein expression examination using western blotting.

### 2.7. Western blotting

Cells were washed with PBS and proteins were extracted using laemmli buffer. Protein concentration was measured using Modified Lowry Protein Assay Kit, (Pierce Biotechnology, Inc.) according to the manufacturer's instructions. 30 μg of proteins were separated using SDS–PAGE. Proteins were transferred to nitrocellulose membrane and the expression of TIP47 and β-actin was evaluated using mouse anti-TIP47 (B3) antibody and mouse anti-β-actin (C4) antibody (Santa Cruz Biotechnology Inc., USA), respectively. Goat anti-mouse IgG-HRP (Santa Cruz Biotechnology Inc., USA) along with TMB Membrane Peroxidase Substrate System (KPL Inc., USA) was used for colorimetric detection of the protein bands.

### 2.8. Lipid droplet staining

A 0.35% oil-red-O (ORO) stock solution (Serva, Germany) was prepared and filtered using a 0.22 μm filter. A working solution of ORO was freshly prepared by diluting the stock solution with double distilled water at a 6:4 ratio, was left to stand for 20 min and filtered using a 0.22 μm filter. Cultured cells were fixed with 4% formaldehyde in PBS for 10 min. Fixed cells were washed with 3 changes of PBS. Cells were permeabilized by incubating with 0.05% Tween 20 in PBS for 15 min followed by 3 washes with PBS then once with 60% isopropanol. Afterwards, cells were incubated with ORO working solution for 10 min followed by 4 washes with distilled water and then mounted with a mounting solution containing DAPI to stain the cell nuclei. LDs and nuclei were visualized using fluorescence microscopy with a 100× objective (Axiom Zeiss).

### 2.9. Viral nucleic acid extraction and quantification

Isolation of the viral RNA from mammalian cells was done using Invisorb Spin Virus RNA Mini Kit (Invitek) according to the manufacturers' instruction. Viral nucleic acid was quantified using viral nucleic acid detection kit (Genesig, Primer design, UK) according to manufacturer's protocol. Absolute quantification was calculated according to standards of known quantities.

### 2.10. Luciferase reporter assay

The pmirGLO vector (Promega) was used to validate the binding of miR-148a and miR-30a to the 3′UTR of TIP47. The binding region of miR-148a and miR-30a in the 3′UTR of TIP47 were designed with sticky ends of SacI and XbaI restriction sites. Sense and antisense oligonucleotides of miR-148a (sense: 5′-CTCAGCGGGCCCCG TCTCTATAA**TGCAGCTG**TGCTCTGGAT-3′, antisense: 5′-CTAGATCC AGAGCA**CAGCTGCA**TTATAGAGACGGGGCCCGCTGA GAGCT-3′) or miR-30a (sense: 5′-CTAGTTCATATCCCACTTCTT**TGTTTAC**ACCGA TT-3′, antisense 5′-CTAGAATCGGT**GTAAACA**AAGAAGTGGGATATG AACTAGAGCT-3′) binding regions were annealed and cloned into pmirGLO vector between SacI and XbaI restriction sites (WT-148 and WT-30, respectively). A mutant type vector of each binding region with deletion of the region complementary to the seed sequence of each of the miRNAs in the 3′UTR of TIP47 (underlined in the above sequences) was constructed (Mut-148 and Mut-30).

Huh7 cells were transfected with 1 μg of either WT-148, Mut-148, WT-30 or Mut-30 vectors using Superfect transfection reagent (Qiagen). After 24-h cells were transfected with miR-148a or miR-30a mimics using Hiperfect transfection reagent (Qiagen). 48-h post transfection luciferase activity was measured using Steady-Glo luciferase Assay system (Promega).

### 2.11. Statistical analysis

Data are expressed as mean ± standard error of the mean and were analyzed using Student *T* test using GraphPad Prism 5. *P* values lower than 0.05 were considered statistically significant.

## 3. Results

### 3.1. Bioinformatics analysis

Potential microRNAs that target the 3′ untranslated region (3′UTR) of TIP47 were identified using the bioinformatics tools miRanda, TargetScan and mirDIP. Selection of microRNAs to be investigated in this study was based on their predicted mirSVR binding scores to TIP47. mirSVR scoring takes into account various features of the predicted miRNA:mRNA duplex, including base pairing at the seed region, A/U composition near the target sites, secondary structure accessibility, length of the UTR and relative position of the target site in the UTR. mirSVR scores correlate linearly with the extent of downregulation with a suggested score cutoff of −0.1 or lower [16]. MicroRNAs that showed potential binding were compared with the results of a high content assay, performed by Whittaker and colleagues that identified microRNAs that regulate LDs in human hepatocytes [17]. Based on that, miR-30a-5p and miR-148a-3p were selected. miR-30a-5p was found to target the 3′UTR of TIP47 with a mirSVR score of −1.0251, while miR-148a-3p showed a mirSVR score of −0.1210.

### 3.2. Expression profile of TIP47, miR-148a and miR-30a in liver biopsies of HCV infected patients compared to healthy controls

Expression profile of TIP47, miR-148a and miR-30a was investigated in liver biopsies of HCV infected patients compared to healthy controls. TIP47 was found to be upregulated

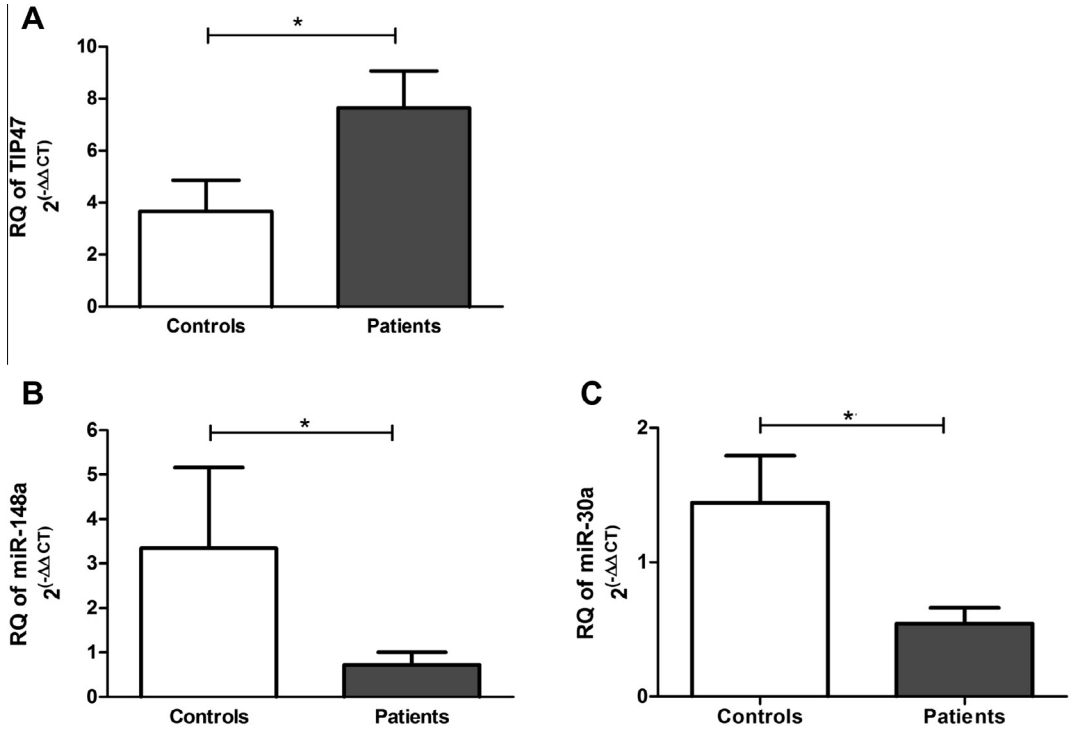


**Fig. 1.** Expression profile of TIP47, miR-148a and miR-30a in liver biopsies of HCV infected patients. (A) TIP47 is upregulated (7.634 ± 1.419, $N = 21$, $P = 0.0489^{*}$) in HCV liver biopsies compared to healthy controls (3.660 ± 1.201, $N = 9$). (B) miR-148a (0.7188 ± 0.2852, $N = 21$, $P = 0.0216^{*}$) and (C) miR-30a (0.5408 ± 0.1183, $N = 21$, $P = 0.0041^{**}$) are downregulated in HCV infected patients compared to healthy controls (3.345 ± 1.814, $N = 9$) and (1.442 ± 0.3492, $N = 9$), respectively. Results are expressed as mean ± S.E.M.

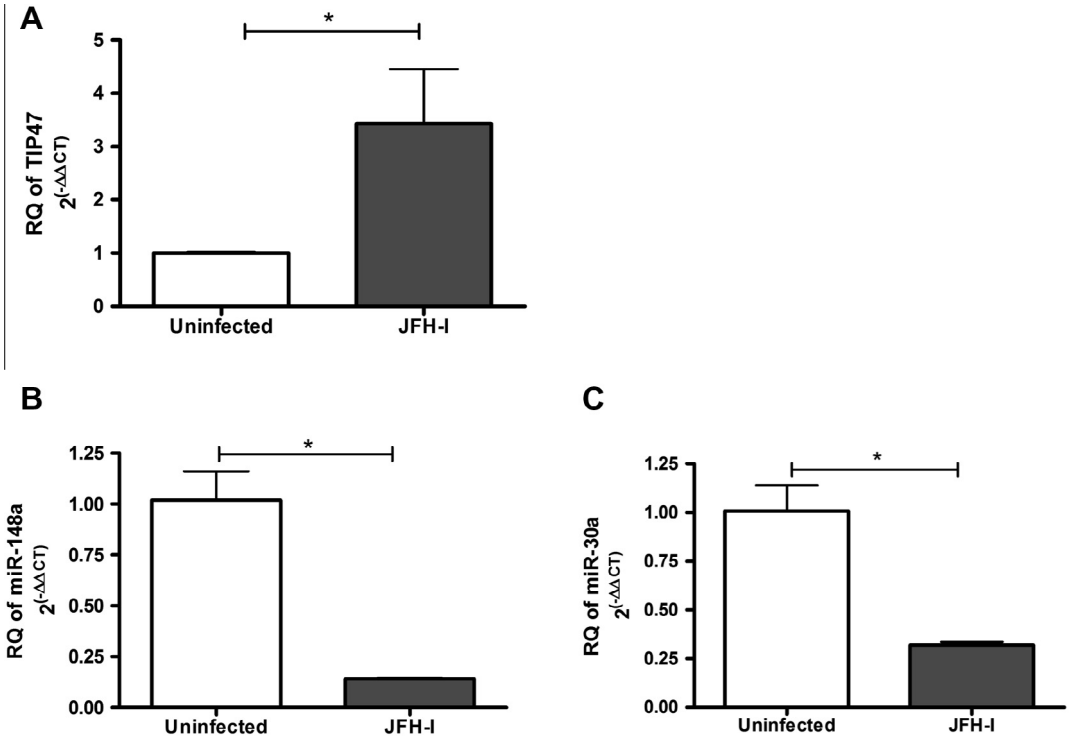


**Fig. 2.** Impact of HCV infection on TIP47, miR-148a and miR-30a expression in Huh7 cells. Infection of Huh7 cells with HCVcc-JFH-I lead to (A) induction of TIP47 expression (3.431 ± 1.027, $P = 0.0167^{*}$) compared to uninfected cells (1.001 ± 0.02294) and suppression of (B) miR-148a (0.1418 ± 0.004423, $P = 0.0172^{*}$) and (C) miR-30a (0.3201 ± 0.01441, $P = 0.0353^{*}$) compared to naïve cells (1.019 ± 0.1416) and (1.009 ± 0.1321), respectively. Results are expressed as mean ± S.E.M., $n = 4$.

($P = 0.0489^{*}$), while miR-148a and miR-30a were downregulated ($P = 0.0216^{*}$ and $P = 0.0041^{**}$, respectively) in HCV patients (Fig. 1).

### 3.3. Expression profile of TIP47, miR-148a and miR-30a in JFH-1 infected Huh7 cell lines

To confirm that the observed alteration in TIP47 and microRNAs expression in patients' biopsies is due to HCV infection, Huh7 cells were infected with HCVcc-JFH-I and TIP47, miR-148a and miR-30a expression was compared to uninfected cells. Infection of Huh7 cell lines resulted in induction of TIP47 ($P = 0.0167^{*}$) and suppression of miR-148a and miR-30a expression compared to uninfected cells (Fig. 2).

### 3.4. Impact of manipulating miR-148a and miR-30a on TIP47 mRNA & protein expression

miR-148a and miR-30a mimics or antagomirs were transfected 3 days post infection of Huh7 cells with JFH-I. siRNAs against TIP47 were also transfected as a positive control. 24-h post transfection, cells were treated with OA to induce LD formation. 48 h and 72 h post OA treatment TIP47 mRNA and protein expression, respectively, was examined. Efficient transfection of mimics was confirmed by measuring microRNA expression in transfected compared to mock cells, where miR-148a increased by a mean of 800 folds ($P = 0.0232^{*}$), while miR-30a expression was increased by a mean of 1500 folds ($P = 0.0002^{***}$) in mimicked compared to mock cells (Fig. 3A and B).

miR-148a and miR-30a mimics suppressed TIP47 mRNA ($P = 0.0488^{*}$ and $P = 0.0262^{*}$, respectively) and protein expression compared to untransfected cells (1.017 ± 0.09644). miR-148a and miR-30a antagomirs did not significantly affect TIP47 mRNA or protein expression. siRNAs against TIP47 efficiently suppressed its mRNA ($P = 0.0002^{***}$) and protein expression (Fig. 3C and D; SI Fig. 1).

### 3.5. Validation of miR-148a and miR-30a binding to 3′UTR of TIP47

To validate that miR-148a and miR-30a induce their suppressive effects on TIP47 by directly binding to its 3′UTR, wild type or mutant binding regions of miR-148a or miR-30a were cloned downstream of luciferase reporter gene in pmirGLO vector (Fig. 4A and B). The designed constructs were transfected in Huh7 cells followed by transfection of miR-148a or miR-30a mimics. Luciferase activity was measured 48 h post transfection. miR-148a mimics suppressed luciferase activity in cells harboring the miR-148a wild type construct (WT-148) ($P = 0.0194^{*}$) but did not affect the activity in cells harboring the mutant vector (Mut-148) (Fig. 4C). Similarly, miR-30a mimics suppressed luciferase activity in cells harboring wild type miR-30a vector (WT-30) ($P = 0.04138^{*}$) but not the mutant type (Mut-30) (Fig. 4D).

### 3.6. Impact of manipulating miR-148a and miR-30a expression on cellular lipid droplet content

The effect of manipulating miR-148a and miR-30a on cellular lipid droplets was studied by staining LDs with oil-red-O dye and visualizing them using fluorescence microscopy. Cellular lipid droplet content decreased upon transfection of miR-148a and miR-30a mimics, while their antagomirs did not markedly affect the cellular LDs. TIP47 siRNAs also decreased LD levels (Fig. 5).

### 3.7. Impact of manipulating miR-148a and miR-30a expression on HCV JFH-I viral load

Forcing the expression of miR-148a and miR-30a lead to a mean decrease of 36% ($P = 0.0401^{*}$) and 50% ($P = 0.0475^{*}$), respectively, in the viral load (VL) in JHF-I infected, OA treated Huh7 cells compared to mock cells. The VL was not significantly affected upon antagonizing either miR-148a or miR-30a. Knock down of TIP47

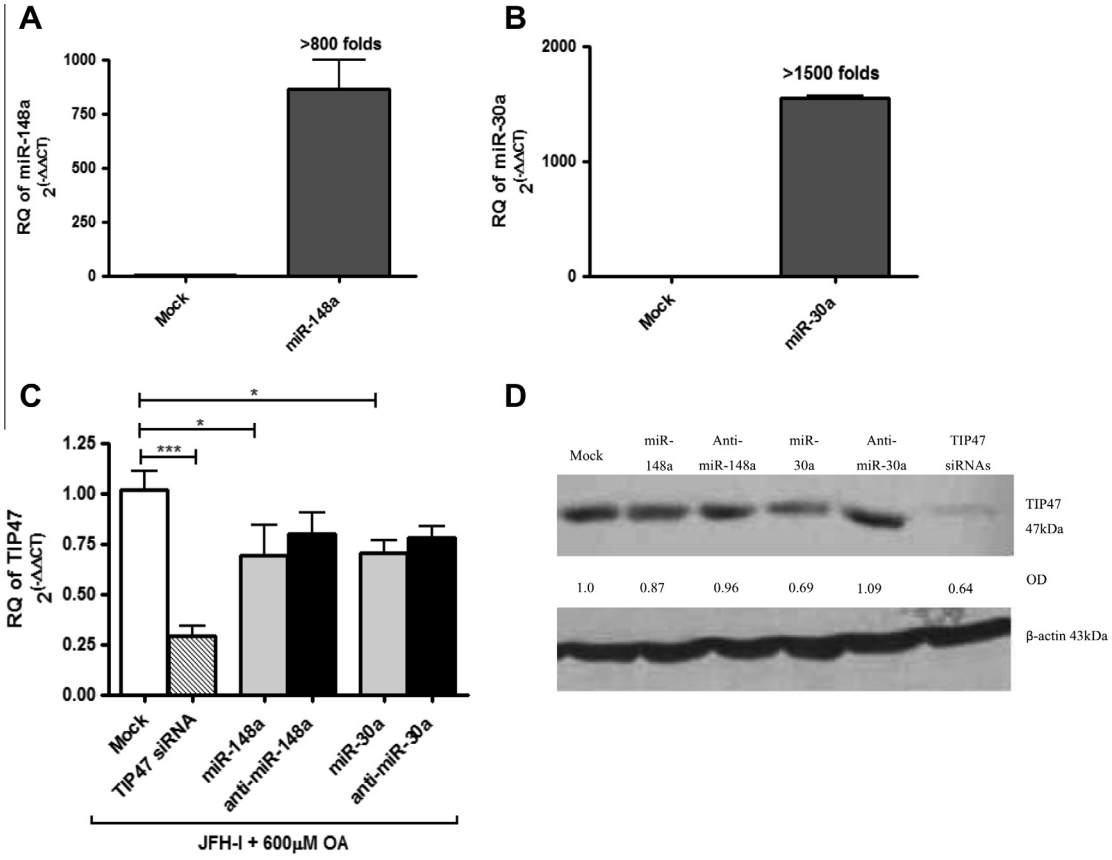


**Fig. 3.** Impact of manipulating miR-148a and miR-30a on TIP47 mRNA and protein expression in JFH-I infected Huh7 cells. Efficient delivery of miR-148a (A) and miR-30a (B) mimics into Huh7 cells was confirmed by measuring microRNA relative quantity in transfected compared to untransfected cells. miR-148a increased by ~800 folds and miR-30a increased by ~1500 folds in mimicked compared to untransfected cells. (C) miR-148a and miR-30a mimics suppressed TIP47 mRNA expression (0.6906 ± 0.1489, $P = 0.0488^{*}$) and (0.7016 ± 0.06406, $P = 0.0262^{*}$), respectively, compared to mock cells (1.017 ± 0.09644). siRNAs against TIP47 efficiently suppressed its expression (0.2910 ± 0.05208, $P = 0.0002^{***}$). Results are expressed as mean ± S.E.M., $n = 5$. (D) Protein expression of TIP47 was suppressed by miR-148a (0.87), miR-30a (0.69) and TIP47 siRNAs (0.64). Results are expressed as relative density of TIP47 bands compared to mock cells.

with siRNAs decreased the VL by a mean of 49% ($P = 0.0291^{*}$) (Fig. 6).

## 4. Discussion

Lipid droplets act as an assembly platform for HCV and thus play an important role in the viral life cycle [3,18]. LDs formation and stabilization is controlled by a number of proteins associated to their surfaces among which are the PAT proteins [19,20]. Alteration in cellular LD content as well as their associated PAT protein, TIP47, was previously shown to affect HCV replication and assembly [5,11,12]. However, the regulation of PAT proteins by microRNAs and how they would affect HCV infection has never been investigated. Thus, this study focused on investigating the microRNA regulation of hepatic TIP47 expression, in an attempt to decrease LDs and subsequently attenuate HCV infection. MicroRNAs that potentially target TIP47 were identified using bioinformatics analysis. In 2010, a group in California performed a high content screening assay to identify microRNAs that regulate hepatic LDs [17]. To select microRNAs to be investigated in this study, the results of the bioinformatics analysis were compared to those of the high content screen. Two microRNAs, miR-148a and miR-30a were selected for this study as they were shown by bioinformatics to target TIP47 and were also reported by the Whittaker study to regulate LDs [17]. The impact of HCV infection on hepatic TIP47 and microRNA expression was investigated by measuring their expression in liver biopsies of HCV infected patients and healthy controls using qRT-PCR. TIP47 was found to be upregulated (Fig. 1A), while miR-148a and miR-30a were downregulated (Fig. 1B and C) in HCV infected biopsies. However, no correlation was observed between the expression of TIP47 and either of the microRNAs. To confirm that the observed alteration in TIP47 and microRNA expression in liver biopsies is due to HCV infection, the impact of infecting Huh7 cells with HCVcc-JFH-I on TIP47, miR-148a and miR-30a expression was investigated. Interestingly, the same expression pattern as in liver biopsies of HCV infected patients was observed, where TIP47 was induced, while miR-148a and miR-30a were suppressed upon infection of Huh7 cells (Fig. 2). These results are in accordance with a study that reported that TIP47 expression was higher in HepG2 cells expressing HCV core protein compared to cells not expressing the core protein [5]. Another study showed that TIP47 mRNA expression was higher in HCV infected Huh7.5 cells as well as primary hepatocytes [11].

Since miR-148a and miR-30a were downregulated in HCV infected patients, it was interesting to examine whether correcting their expression using specific oligos would affect the expression of their predicted downstream target TIP47. Hence, JFH-I infected Huh7 cells were transfected with miR-148a or miR-30a mimics or antagomirs or specific siRNAs against TIP47 as a positive control. 24 h after transfection, cells were treated with OA, an inducer of LDs, to determine the effect of both microRNAs on LD formation.

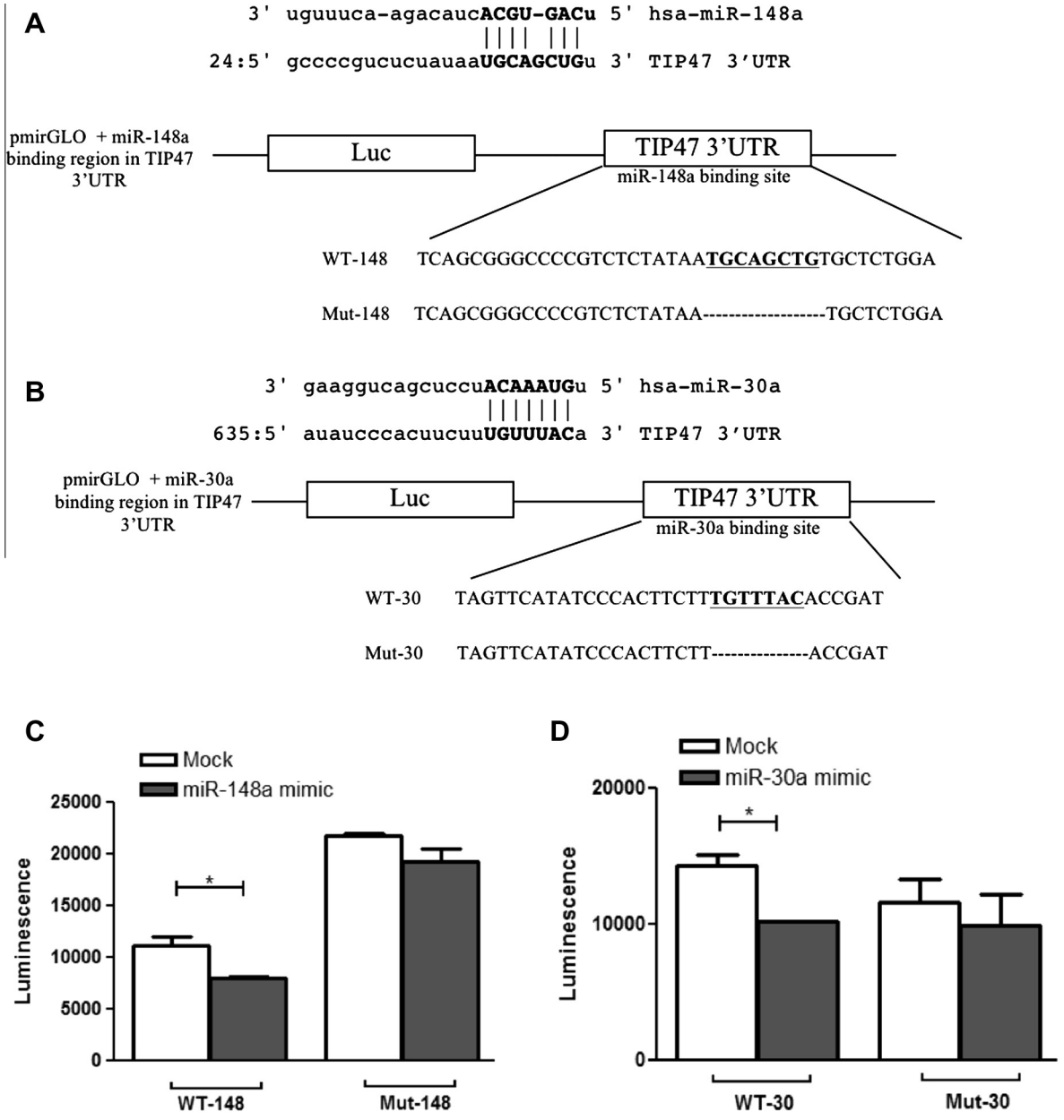


**Fig. 4.** Validation of miR-148a and miR-30a binding to 3′UTR of TIP47. (A) Sequence alignment of miR-148a and the 3′ UTR of TIP47 and the construction of pmirGLO vector harboring either wild type miR-148a binding region (WT-148) or a mutant type binding region in which the seed region of miR-148a was deleted (Mut-148). (B) Sequence alignment of miR-148a and the 3′ UTR of TIP47 and the construction of pmirGLO vector harboring either wild type miR-30a binding region (WT-30) or a mutant type binding region in which the seed region of miR-30a was deleted (Mut-30). (C) miR-148a mimics suppressed the luciferase activity in cells harboring WT-148 vector ($P = 0.0194^*$), but did not affect its activity in cells harboring Mut-148. (D) miR-30a mimics suppressed the luciferase activity in cells harboring WT-30 vector ($P = 0.0413^*$), but did not affect its activity in cells harboring Mut-30. Results are expressed as mean ± S.E.M., $n = 3$.

TIP47 mRNA and protein expression were examined 48 and 72 h, respectively, post OA treatment. Interestingly, both miR-148a and miR-30a mimics suppressed TIP47 expression on the mRNA and protein level (Fig. 3C and D; SI Fig. 1). This shows that TIP47 could indeed be a downstream target of both microRNAs as predicted by bioinformatics. Thus, the direct targeting of miR-148a and miR-30a to TIP47 3′UTR was investigated and confirmed through performing luciferase reporter assay, where miR-148a and miR-30a suppressed luciferase activity in cells transfected with pmirGLO vector harboring miR-148a or miR-30a binding regions on TIP47 3′UTR (Fig. 4C and D).

The impact of manipulating miR-148a and miR-30a on cellular LDs was then examined by staining LDs with oil-red-O 72 h post OA treatment. miR-148a and miR-30a mimics decreased LDs compared to mock cells, which was also observed in TIP47 knockdown cells (Fig. 5). This decrease in LDs could be in part due to suppression of TIP47, since previous reports showed that TIP47 is involved in LD biogenesis and that knock down of TIP47 inhibited growth and maturation of LDs [21]. Moreover, in vivo tests showed that knock down of TIP47 using antisense oligonucleotides improved hepatic steatosis in high-fat fed mice [22].

Since LDs were repeatedly reported to play an important role in HCV life cycle, it was intriguing to investigate whether the decrease in LDs and TIP47 in response to forcing the expression of miR-148a and miR-30a would also repress HCV replication. Interestingly, miR-148a and miR-30a mimics were found to

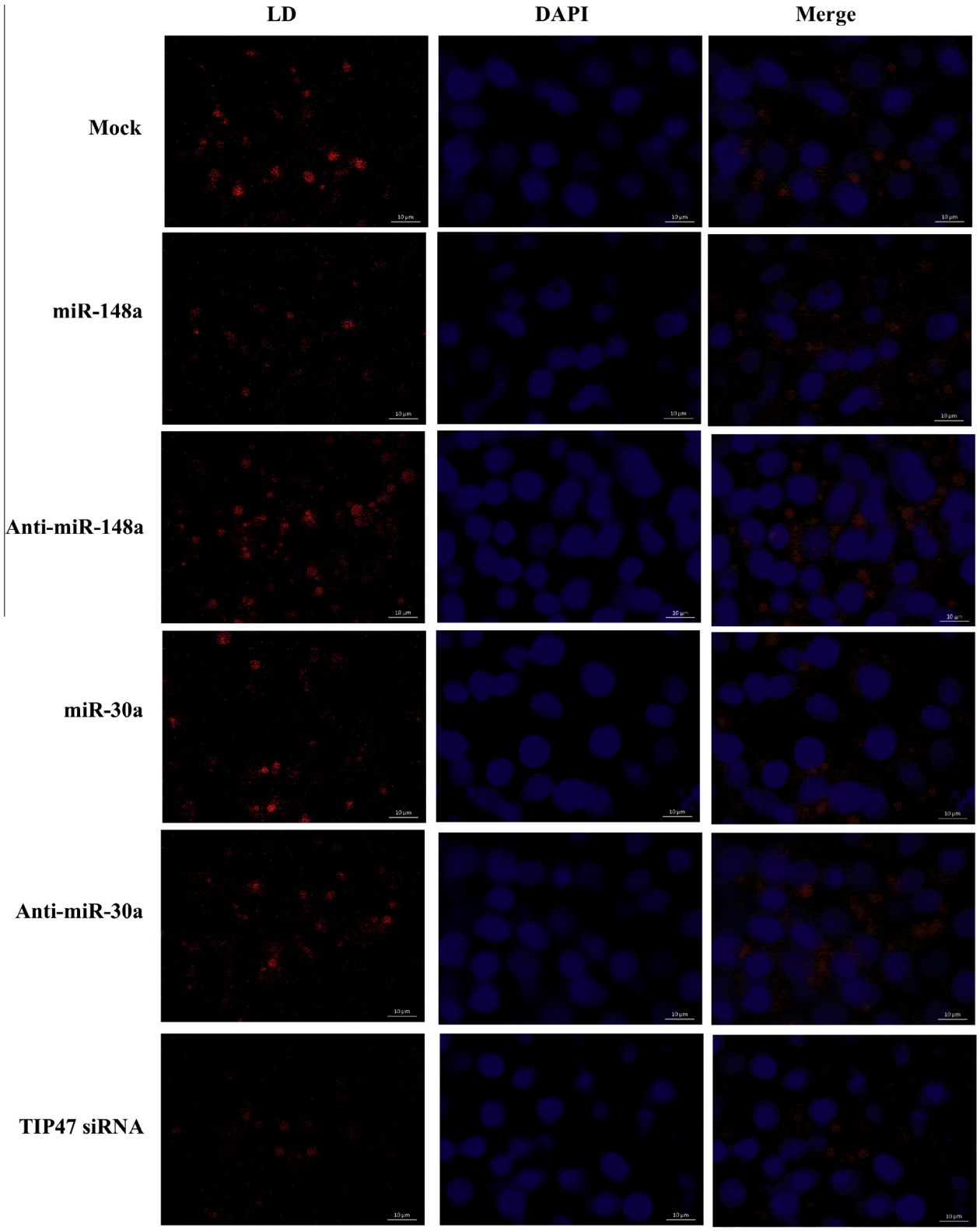


**Fig. 5.** Impact of miR-148a and miR-30a on cellular LDs. miR-148a and miR-30a mimics decreased LDs in Huh7, OA treated cells compared to mock cells. miR-148a and miR-30a antagomirs did not markedly affect LDs. TIP47 siRNAs lead to a decrease in cellular LDs. Red fluorescence represents lipid droplets stained with oil-red-O. Blue fluorescence represents the cell nuclei stained with DAPI. Scale bars are equal to 10 μm.

decrease viral RNA by 36% and 50%, respectively. The decrease in viral RNA in response to miRNA mimics was similar to the decrease induced by TIP47 siRNAs, where TIP47 knockdown lead to a 49% decrease in viral RNA (Fig. 6). These findings go along with two recent studies, which showed that knockdown of TIP47 resulted in a marked suppression of HCV replication and release of infectious viral particles [11,12]. Similar to our findings, another study showed that overexpression of miR-27a

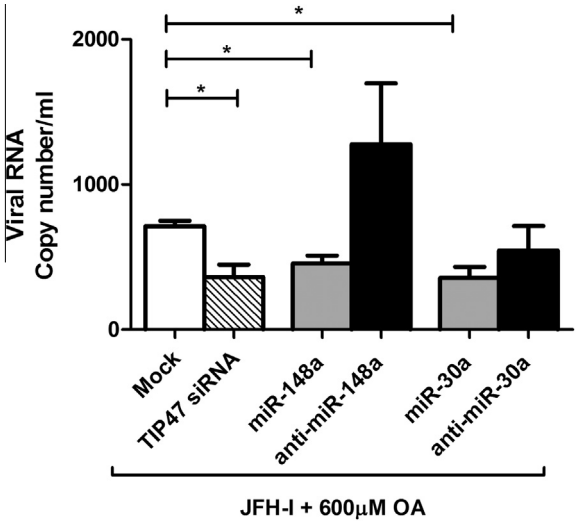


**Fig. 6.** Impact of manipulating miR-148a and miR-30a expression on HCV JFH-I viral load. Effect of manipulating miR-148a and miR-30a in JFH-I infected, OA treated cells on the intracellular viral load was examined. miR-148a and miR-30a mimics decreased the VL by 36% (456.3 ± 52.55, $P = 0.0401^*$) and 50% (355.1 ± 77.95, $P = 0.0475^*$), respectively, compared to mock cells (711.5 ± 37.50). miR-148a and mir-30a antagomirs did not affect the VL significantly. TIP47 knockdown decreased VL by a mean of 49% (362.3 ± 84.50, $P = 0.0291^*$) compared to mock cells. Results are expressed as mean ± S.E.M., $n = 5$.

resulted in repression of LDs as well as HCV replication in Huh7.5 cells [15].

In conclusion the collective findings of this study show that HCV infection induces hepatic TIP47 expression. Moreover, HCV infection suppresses miR-148a and miR-30a expression. Forcing the expression of miR-148a and miR-30a suppressed TIP47 mRNA and protein expression and hence decreased cellular LDs as well as intracellular HCV RNA. Thus, miR-148a and miR-30a reversed the effects induced by HCV infection and could be used as potential therapeutic targets to attenuate HCV infection and treat hepatic steatosis induced by HCV.

## Acknowledgments

We would like to acknowledge Prof. Takaji Wakita for kindly providing us with the pJFH-I construct.

All authors have read the journal's policy and there are no conflicts of interests to declare.

## Appendix A. Supplementary data

Supplementary data associated with this article can be found, in the online version, at http://dx.doi.org/10.1016/j.febslet.2015.06.040.

## References

[1] Su, A.I., Pezacki, J.P., Wodicka, L., Brideau, A.D., Supekova, L., Thimme, R., Wieland, S., Bukh, J., Purcell, R.H., Schultz, P.G. and Chisari, F.V. (2002) Genomic analysis of the host response to hepatitis C virus infection. Proc. Natl. Acad. Sci. USA 99, 15669–15674.

[2] Siagris, D., Christofidou, M., Theocharis, G.J., Pagoni, N., Papadimitriou, C., Lekkou, A., Thomopoulos, K., Starakis, I., Tsamandas, A.C. and Labropoulou-Karatza, C. (2006) Serum lipid pattern in chronic hepatitis C: histological and virological correlations. J. Viral Hepatitis 13, 56–61.

[3] Miyanari, Y., Atsuzawa, K., Usuda, N., Watashi, K., Hishiki, T., Zayas, M., Bartenschlager, R., Wakita, T., Hijikata, M. and Shimotohno, K. (2007) The lipid droplet is an important organelle for hepatitis C virus production. Nat. Cell Biol. 9, 1089–1097.

[4] Gosert, R., Egger, D., Lohmann, V., Bartenschlager, R., Blum, H.E., Bienz, K. and Moradpour, D. (2003) Identification of the hepatitis C virus RNA replication complex in Huh-7 cells harboring subgenomic replicons. J. Virol. 77, 5487–5492.

[5] Sato, S., Fukasawa, M., Yamakawa, Y., Natsume, T., Suzuki, T., Shoji, I., Aizaki, H., Miyamura, T. and Nishijima, M. (2006) Proteomic profiling of lipid droplet proteins in hepatoma cell lines expressing hepatitis C virus core protein. J. Biochem. 139, 921–930.

[6] Gonzalez-Peralta, R.P., Fang, J.W., Davis, G.L., Gish, R., Tsukiyama-Kohara, K., Kohara, M., Mondelli, M.U., Lesniewski, R., Phillips, M.I., Mizokami, M., et al. (1994) Optimization for the detection of hepatitis C virus antigens in the liver. J. Hepatol. 20, 143–147.

[7] Boulant, S., Targett-Adams, P. and McLauchlan, J. (2007) Disrupting the association of hepatitis C virus core protein with lipid droplets correlates with a loss in production of infectious virus. J. Gen. Virol. 88, 2204–2213.

[8] Wolins, N.E., Skinner, J.R., Schoenfish, M.J., Tzekov, A., Bensch, K.G. and Bickel, P.E. (2003) Adipocyte protein S3–12 coats nascent lipid droplets. J. Biol. Chem. 278, 37713–37721.

[9] Yamaguchi, T., Matsushita, S., Motojima, K., Hirose, F. and Osumi, T. (2006) MLDP, a novel PAT family protein localized to lipid droplets and enriched in the heart, is regulated by peroxisome proliferator-activated receptor alpha. J. Biol. Chem. 281, 14232–14240.

[10] Miura, S., Gan, J.W., Brzostowski, J., Parisi, M.J., Schultz, C.J., Londos, C., Oliver, B. and Kimmel, A.R. (2002) Functional conservation for lipid storage droplet association among Perilipin, ADRP, and TIP47 (PAT)-related proteins in mammals, Drosophila, and Dictyostelium. J. Biol. Chem. 277, 32253–32257.

[11] Ploen, D., Hafirassou, M.L., Himmelsbach, K., Sauter, D., Biniossek, M.L., Weiss, T.S., Baumert, T.F., Schuster, C. and Hildt, E. (2013) TIP47 plays a crucial role in the life cycle of hepatitis C virus. J. Hepatol. 58, 1081–1088.

[12] Vogt, D.A., Camus, G., Herker, E., Webster, B.R., Tsou, C.L., Greene, W.C., Yen, T.S. and Ott, M. (2013) Lipid droplet-binding protein TIP47 regulates hepatitis C Virus RNA replication through interaction with the viral NS5A protein. PLoS Pathog. 9, e1003302.

[13] Ploen, D., Hafirassou, M.L., Himmelsbach, K., Schille, S.A., Biniossek, M.L., Baumert, T.F., Schuster, C. and Hildt, E. (2013) TIP47 is associated with the hepatitis C virus and its interaction with Rab9 is required for release of viral particles. Eur. J. Cell Biol. 92, 374–382.

[14] Singaravelu, R., Chen, R., Lyn, R.K., Jones, D.M., O'Hara, S., Rouleau, Y., Cheng, J., Srinivasan, P., Nasheri, N., Russell, R.S., Tyrrell, D.L. and Pezacki, J.P. (2014) Hepatitis C virus induced up-regulation of microRNA-27: a novel mechanism for hepatic steatosis. Hepatology 59, 98–108.

[15] Shirasaki, T., Honda, M., Shimakami, T., Horii, R., Yamashita, T., Sakai, Y., Sakai, A., Okada, H., Watanabe, R., Murakami, S., Yi, M., Lemon, S.M. and Kaneko, S. (2013) MicroRNA-27a regulates lipid metabolism and inhibits hepatitis C virus replication in human hepatoma cells. J. Virol. 87, 5270–5286.

[16] Betel, D., Koppal, A., Agius, P., Sander, C. and Leslie, C. (2010) Comprehensive modeling of microRNA targets predicts functional non-conserved and non-canonical sites. Genome Biol. 11, R90.

[17] Whittaker, R., Loy, P.A., Sisman, E., Suyama, E., Aza-Blanc, P., Ingermanson, R.S., Price, J.H. and McDonough, P.M. (2010) Identification of MicroRNAs that control lipid droplet formation and growth in hepatocytes via high-content screening. J. Biomol. Screen. 15, 798–805.

[18] Negro, F. and Sanyal, A.J. (2009) Hepatitis C virus, steatosis and lipid abnormalities: clinical and pathogenic data. Liver Int. 29 (Suppl. 2), 26–37.

[19] Londos, C., Sztalryd, C., Tansey, J.T. and Kimmel, A.R. (2005) Role of PAT proteins in lipid metabolism. Biochimie 87, 45–49.

[20] Martin, S. and Parton, R.G. (2006) Lipid droplets: a unified view of a dynamic organelle. Nat. Rev. Mol. Cell Biol. 7, 373–378.

[21] Bulankina, A.V., Deggerich, A., Wenzel, D., Mutenda, K., Wittmann, J.G., Rudolph, M.G., Burger, K.N. and Honing, S. (2009) TIP47 functions in the biogenesis of lipid droplets. J. Cell Biol. 185, 641–655.

[22] Carr, R.M., Patel, R.T., Rao, V., Dhir, R., Graham, M.J., Crooke, R.M. and Ahima, R.S. (2012) Reduction of TIP47 improves hepatic steatosis and glucose homeostasis in mice. Am. J. Physiol. Regul. Integr. Comp. Physiol. 302, R996–1003.